Submitted to *Decision Analysis*
manuscript (Please, provide the manuscript number!)

Value of Information Analysis for Complex Simulator Models: Application to Wind Farm Maintenance

Hans Olav Vogt Myklebust
Department of Mathematical Sciences, NTNU, Norway, hans.olav.vm@gmail.com

Jo Eidsvik
Department of Mathematical Sciences, NTNU, Norway, jo.eidsvik@ntnu.no

Iver Bakken Sperstad
SINTEF Energy Research, Trondheim, Norway, iver.bakken.sperstad@sintef.no

Debarun Bhattacharjya
Research AI, IBM T.J. Watson Research Center, New York, US, debarunb@us.ibm.com

Many domains require the use of sophisticated simulators to adequately model the effect of chosen alternatives on the decision maker's value. Decision support in such complex systems brings unique challenges around efficiency, since simulating each combination of inputs can be time-consuming. In this paper, we conduct a value of information (VOI) analysis to study whether one should purchase information about critical input uncertainties in such complex systems. We propose a novel computational approach where Gaussian processes are used to model the decision maker's profit as a function of different alternatives and uncertainties. Under this modeling assumption, the expected improvement of the profit is analytically available, which we use to approximate the VOI effectively over batches of simulations, thus avoiding too many computer intensive evaluations of the system. We illustrate the proposed computational approach with an offshore wind farm maintenance application, where the decision maker relies on outputs from large-scale simulations to determine the optimal vessel fleet mix and number of personnel for operation and maintenance. Such computer intensive simulations mimic long-term energy production under different input conditions. It is often not possible to explore all the alternatives exhaustively, and one must therefore guide the simulations to run on promising alternatives. We conduct a VOI analysis to study whether one should purchase information about failure rates of wind turbines, for this application. The proposed methodologies are general and apply to other domains involving expensive simulators.

Key words: value of information, simulation, expected improvement, Gaussian processes, wind farms, failure rates

1. Introduction

The use of computationally expensive simulation tools in decision support is increasingly recognized across industries and fields of science (Ghanem et al. 2017, Owen et al. 2017). Modeling complex decision situations often requires the use of such simulators so as to adequately represent the interactions in the real world and hence avoid making decisions based on biased or erroneous calculations.

In this paper, we highlight the challenges of performing value of information (VOI) analysis when computing values as a function of the inputs (alternatives and states of uncertainties) is time-consuming. We propose a computational approach that relies on Bayesian optimization (BO) for efficient assessment of alternatives and for the associated computations required for VOI analysis of the uncertainty under consideration. BO has been shown to be useful in situations where expensive simulators are required to evaluate an output, see e.g. Frazier and Wang (2016). Like in that work, we approximate the relationship between inputs and the output value of a simulator with a Gaussian process (GP), where the mean and covariance structures are adjusted after each (batch of) computer simulation(s), but our approach goes beyond the optimization and effectively constructs an approximation for the VOI. GPs are popular for approximating unknown functions because of their flexibility in handling input variables, ease of interpretation from mean and covariance parameterization, and computational tractability which enables fast selection of simulation evaluation points (Gramacy and Lee 2009, Roustant et al. 2012).

VOI is a concept that has a long history in decision analysis (Howard 1966, Matheson 1968) and VOI analysis remains an important part of a decision analyst's toolkit. There is significant literature on VOI analysis for decision making in applications such as health risk management (Yokota and Thompson 2004), oil and gas (Bratvold et al. 2009), portfolio problems (Bhattacharjya et al. 2013), the environmental sciences (Keisler et al. 2014), and broadly in the Earth sciences (Eidsvik et al. 2015). VOI analysis has not however received much attention in the context of complex simulator models, most likely because of the computational challenges of conducting value evaluations and optimization routines for different data. We hence expand the applicability of VOI analysis to complex settings in this work, by presenting new approximation methods.

The methodologies presented in this paper are motivated by an application involving the operation and maintenance (O&M) of offshore wind farms (Tavner 2012). A survey from Welte et al. (2018) indicated that the O&M cost of an offshore farm lies between 12-32% of its total Levelized Cost of Energy (LCOE), and according to a report from the International Renewable Energy Agency, the LCOE for offshore wind turbines is 2.3 times higher than that of onshore wind turbines (IRENA 2018). For offshore wind power to be competitive with other sources of renewable energy, the costs related to O&M must hence be reduced. We study the optimization of O&M strategies

in this setting, where a decision maker chooses a vessel fleet mix for transferring maintenance personnel (technicians) to turbines after failure. Such decision situations need to deal with the large size of the alternative space and the large simulation time required to evaluate the realized O&M costs for a considered alternative. Matters are further complicated by uncertainties related to the failure rate of components. Here we conduct a VOI analysis to study the economic value of learning this failure rate before making the strategic O&M decision. This elaborate case study brings pedagogical clarity to the application of sophisticated computational approaches for VOI analysis by illustrating the steps for a simple but practical example.

The remainder of the paper is organized as follows. In Section 2, a decision-analytic formulation is specified. In Section 3, BO is discussed, using GPs as surrogate models to efficiently design evaluation points for the next iteration of the optimization procedure. In Section 4, this iterative optimization algorithm is extended to the context of VOI approximation. Here we provide details of the proposed approach for efficient VOI computation with expensive simulators. In Section 5, results on the case study with O&M strategies for offshore wind farms are presented. Finally, we conclude in Section 6.

2. Background

2.1. Complex Simulators for Decision Support

There has long been an interest in designing experiments, conducting sensitivity analysis to input parameters, and studying the value of learning uncertainties in decision models that involve expensive simulation computations (Sacks et al. 1989, Oakley and O'Hagan 2004, Strong et al. 2015). In this paper we consider decision making and VOI analysis for situations that require complex simulations to assess the value function.

The motivating application for this work is offshore wind power generation which is a young industry characterized by limited operational experience, large uncertainties and costs that are declining but still relatively high. In contrast to onshore wind farms, offshore wind farm involves complex marine logistics. Without an effective O&M strategy, logistics delays may cause long downtimes after turbine failures and correspondingly large energy production losses that may threaten the profitability of the wind farm project. Energy profits from offshore wind farm projects are usually estimated via simulation experiments that mimic wind turbine activity, including turbine failures and associated maintenance activities and logistics, along with physical and weather conditions at sea, yielding economic values as output. Several such simulation tools have been developed, see for instance Hofmann (2011), Welte et al. (2018) and Seyr and Muskulus (2019) for overviews. In this paper, we calculate costs and profits using the NOWIcob (**N**orwegian **o**ffshore **wi**nd power life cycle **co**st and **b**enefit) simulation model (Hofmann and Sperstad 2013, Sperstad et al. 2017a), see Section 5.

The methodologies proposed here are also relevant for other applications involving planning and design in the context of expensive computer experiments. For instance, the approach could be used for models involving simulators in the Earth sciences that mimic physical processes in geology, hydrology and related subjects (Eidsvik et al. 2015). It is too time consuming in such settings to run the simulator for all possible inputs, and instead one must choose the input parameters wisely, and this choice is often done using a surrogate model. Within this application domain, Asher et al. (2015) provide a review of existing approaches building on complex simulators for groundwater modeling. An emerging industry within the same domain is that of subsurface CO2 storage, with complex decision making under multivariable uncertainties and with risks related to potential leakage. Pawar et al. (2016) use simulations over time to study risks associated with several alternatives for CO2 storage, without doing any formal VOI analysis. The methods outlined in the current paper would also be suitable for decision support and VOI analysis of potential data sources in the context of traffic simulation systems (Bierlaire 2015) and large-scale stochastic simulations or discrete event simulations of systems over time, such as applied to homeland security models (Blum and Paté-Cornell 2016). Merrick (2009) provides a review of Bayesian simulation from a decision analysis perspective, and calls out the need for research on VOI analysis for decision making using simulation-based models.

2.2. A Decision-Analytic Formulation

We denote the alternatives for the decision situation by $\boldsymbol{a} \in \mathcal{A}$. The cardinality of the set $\mathcal{A}$ is assumed to be relatively large. In the offshore wind farm application, the alternatives pertain to vessel fleet mix and personnel. The main uncertainty is denoted $\lambda \in \Lambda$, which in the wind farm application is an expected long-term failure rate for wind turbines. A discretized sample space is used for ease of evaluations, and we associate the uncertain variable λ with a probability mass function $p(\lambda)$, $\sum_{\lambda \in \Lambda} p(\lambda) = 1$, that represents the decision maker's prior beliefs about λ. We specify this probability mass function in Section 5.

The value function is defined through the *simulator*, and this is denoted by

$$v = v(\boldsymbol{a}, \lambda), \quad \lambda \in \Lambda, \quad \boldsymbol{a} \in \mathcal{A}. \tag{1}$$

In the wind farm application, the input variables are processed through an event-based simulation using Monte Carlo sampling of the weather (wave height and wind speed) and the failure occurrence times. The value function over the inputs is then the profit estimated by the simulator, which incorporates both the revenues from energy production as well as the costs of O&M.

In order to choose a strategy, the decision maker optimizes the expected utility. For a risk neutral decision maker, the prior value (PV) of the decision situation, i.e. the value without any additional information, is:

$$\text{PV} = \max_{\boldsymbol{a}\in\mathcal{A}} \{E[v(\lambda, \boldsymbol{a})]\} = \max_{\boldsymbol{a}\in\mathcal{A}} \left\{ \sum_{\lambda\in\Lambda} v(\lambda, \boldsymbol{a}) p(\lambda) \right\}. \tag{2}$$

When facing a decision situation like the one involving the selection of personnel and fleet mix, there is an auxiliary decision related to information gathering. Here it could be very useful to get information about the uncertain failure rate λ. This would lead to a more informed decision that yields a higher value on expectation. We distinguish between perfect and imperfect information, where the former means that we get clairvoyant information on the uncertain quantity λ without any error. With perfect information about λ, the expected posterior value (PoV) is

$$\text{PoV}(\lambda) = E\left(\max_{\boldsymbol{a}\in\mathcal{A}} \{v(\lambda, \boldsymbol{a})\} \right) = \sum_{\lambda\in\Lambda} \max_{\boldsymbol{a}\in\mathcal{A}} \{v(\lambda, \boldsymbol{a})\}\, p(\lambda), \tag{3}$$

where the uncertain information is used in the argument in the PoV to clearly denote the uncertain variable over which the expectation is computed.

The VOI is the price at which the decision maker is indifferent between purchasing the information and not. The price of indifference is thus the maximum amount that the decision maker is willing to pay for the information. For a risk neutral decision maker, the VOI of perfect information is

$$\text{VOI}(\lambda) = \text{PoV}(\lambda) - \text{PV}. \tag{4}$$

With imperfect information, one is only able to observe λ indirectly through l, which is a noise-corrupted measurement of λ. We assume the same sample space for l as for λ, and specify a likelihood model $p(l|\lambda)$ for the measurement. The marginal model for the data becomes $p(l) = \sum_\lambda p(l|\lambda)p(\lambda)$. The posterior model is

$$p(\lambda|l) = \frac{p(l\,|\,\lambda)p(\lambda)}{p(l)}. \tag{5}$$

The expected PoV in this case is then

$$\text{PoV}(l) = E\left(\max_{\boldsymbol{a}\in\mathcal{A}} \{E(v(\lambda, \boldsymbol{a})|l)\} \right) = \sum_{l} \max_{\boldsymbol{a}\in\mathcal{A}} \left\{ \sum_{\lambda\in\Lambda} v(\lambda, \boldsymbol{a}) p(\lambda|l) \right\} p(l), \tag{6}$$

and the VOI with imperfect information is

$$\text{VOI}(l) = \text{PoV}(l) - \text{PV}. \tag{7}$$

Recall that the main computational challenge here is that an evaluation of the value function $v(\boldsymbol{a}, \lambda)$ is very time consuming, because of the complexity of the simulator. For the wind farm

application, it is not feasible to compute all possibilities, because the input space is too large. Instead, one must resort to methods that compute the value function for the most important uncertainties and decision alternatives. Next we use methods from BO to help guide the evaluation points of the simulator, for efficient approximation of the value function and the VOI.

3. Bayesian Optimization with Gaussian Process Surrogates

In our proposed approach, we aim to efficiently map the value function using a surrogate statistical model, and then use the model to approximate the VOI. In this section, we introduce the concepts behind the mapping of values, including:

- A statistical surrogate model for $v(\boldsymbol{a}, \lambda)$. We use a GP model for the value, which requires specification of a mean and covariance function. The GP surrogate model is easily updated when new evaluation points are provided. (Section 3.1.)
- A criterion to design the new evaluation points. We use a notion referred to as expected improvement (EI) to guide the selection of new evaluation points. This is done in a sequential manner, where each step consists of a batch of points that are selected and run by the simulator. (Section 3.2.)

3.1. Gaussian Processes

There are many potential choices for a surrogate model. GPs are perhaps the most popular choice because they allow fast updating of the model representation when new evaluations are done. GPs further directly provide uncertainty quantification for the function approximation (profits in our case). Alternative approaches for surrogate models include, for instance, polynomial regression models (Queipo et al. 2005) and artificial neural networks (Snoek et al. 2015).

A GP is defined as a stochastic process where every finite subset of elements has a multivariate normal distribution (Rasmussen 2004). A GP is fully specified by its mean function and covariance model. In practice one must check the assumptions made about the mean and variance, and the Gaussian distribution (see Section 5.4). In our context the GP is located at alternatives for decision variables $\boldsymbol{a} \in \mathcal{A}$ and uncertainties $\lambda \in \Lambda$, and has response $v(\boldsymbol{a}, \lambda)$. We denote the process at all alternatives and all uncertainties by $\boldsymbol{v} = (v_1, \ldots, v_n)$. Its distribution is assumed to be represented adequately by

$$\boldsymbol{v} \sim \mathcal{GP}(\boldsymbol{\mu}, \boldsymbol{\Sigma}). \tag{8}$$

The mean is set to a constant level; $\boldsymbol{\mu} = \mu_0 1_n$, while the covariance structure in $\boldsymbol{\Sigma}$ depends on the distance between different alternatives and different uncertainties. The choice of covariance function encodes our initial knowledge about the smoothness of the unknown function $\boldsymbol{v}$. Assuming

a constant variance and a squared exponential covariance function, which is commonly used in function applications of BO, see e.g. Roustant et al. (2012), we have covariance entries defined by

$$\mathrm{Cov}(v(\boldsymbol{a},\lambda),v(\boldsymbol{a}',\lambda')) = \sigma^2 \exp\left\{ -\frac{(\lambda-\lambda')^2}{\phi_\lambda^2} - \sum_j \frac{(a_j - a_j')^2}{\phi_{a_j}^2} \right\}. \tag{9}$$

Here, the sum goes over different elements in the alternative set. For the wind farm maintenance application, ϕ_{a_j} indicates the different correlation range for the three decision variables: number of personnel and different types of vessels. In practice, the mean μ_0 and covariance model parameters σ, ϕ_{a_j} and ϕ_λ must be specified from current knowledge, or from the available function evaluations. If the initial batch of evaluation points is small, it will help to update these parameters after subsequent batches. There is existing software for fitting GPs, see e.g. Roustant et al. (2012) and Gramacy (2016). Note that even though the covariance function defined in equation (9) is stationary, it will be non-stationary when we start conditioning on simulator evaluations.

Assume we have evaluated the function at M inputs, and denote the observation set by $\boldsymbol{y}_M = (y_1,\ldots,y_M)$. Here, $y_i = v(\boldsymbol{a}_{(i)},\lambda_{(i)}) + N(0,\tau^2)$ is the profit estimated by the simulator for evaluation number i, with input values $(\boldsymbol{a}_{(i)},\lambda_{(i)})$, $i = 1,\ldots,M$. The Gaussian noise term with standard deviation τ is included to account for uncertainty in the function evaluation, which in our application mainly pertains to varying weather conditions in the simulations and their interaction with the simulated times of failure. Using more compact matrix notation, we can write $\boldsymbol{y}_M = \boldsymbol{A}_M\boldsymbol{v} + N(0,\tau^2\boldsymbol{I})$, where the size $M \times n$ matrix $\boldsymbol{A}_M$ contains 0 and 1 entries, and the 1 entries indicate the sampled indices (1), (2), ..., (M) of $\boldsymbol{v}$. The conditional distribution given this information is a GP with modified mean and covariance:

$$\begin{aligned} \boldsymbol{v}|\boldsymbol{y}_M &\sim \mathcal{GP}(\boldsymbol{\mu}_M, \boldsymbol{\Sigma}_M), \\ \boldsymbol{\mu}_M &= \boldsymbol{\mu} + \boldsymbol{\Sigma}\boldsymbol{A}_M^t(\boldsymbol{A}_M\boldsymbol{\Sigma}\boldsymbol{A}_M^t + \tau^2\boldsymbol{I})^{-1}(\boldsymbol{y}_M - \boldsymbol{A}_M\boldsymbol{\mu}), \\ \boldsymbol{\Sigma}_M &= \boldsymbol{\Sigma} - \boldsymbol{\Sigma}\boldsymbol{A}_M^t(\boldsymbol{A}_M\boldsymbol{\Sigma}\boldsymbol{A}_M^t + \tau^2\boldsymbol{I})^{-1}\boldsymbol{A}_M\boldsymbol{\Sigma}. \end{aligned} \tag{10}$$

The updating described in equation (10) is typically done sequentially, with batches of evaluation points. The conditional mean and covariance form the basis for BO in the next batch.

Example:

Figure 1 illustrates the conditioning on the simplified domain of one decision variable $a \in \{1,\ldots,100\}$ shown in increasing order on the horizontal axis. A simulated true process is plotted in the top display and the goal is to predict and maximize this simulated function $v(a)$. The middle plot shows the $M = 6$ evaluation points as circles, along with the conditional process mean (solid, black) and the prediction interval.

The function is predicted very accurately near the data points. Going away from these evaluation points, the prediction is further from the true function and there is larger uncertainty. The smoothness of the prediction and the widths of the prediction intervals is here determined by the correlation in the function values for similar alternatives.

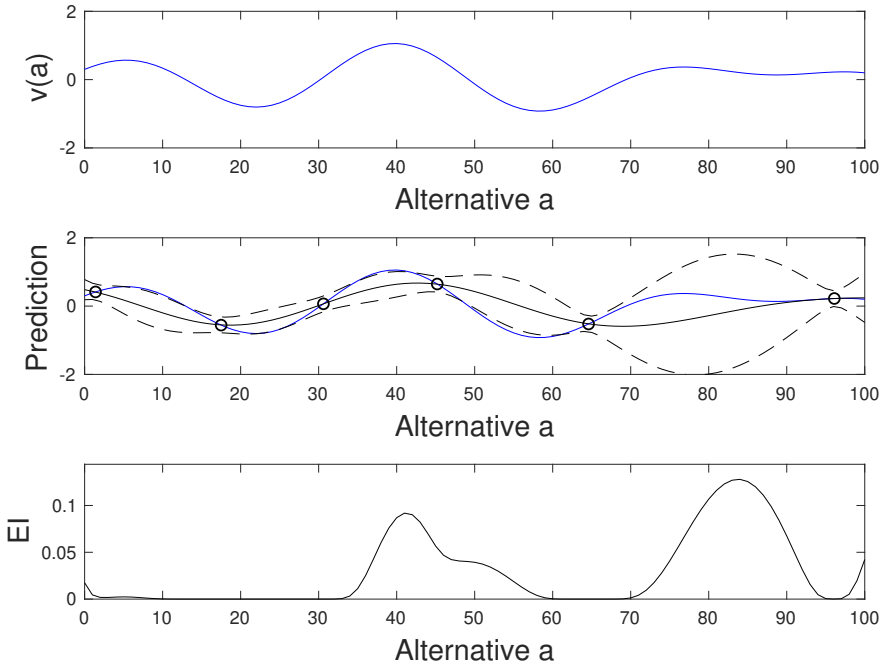

Figure 1 **Top: True function. Middle: Prediction and 90% prediction interval based on GP conditional on six evaluations. Bottom: EI computed from the updated GP model.**

3.2. Expected Improvement

In BO, one uses acquisition functions to help guide the selection of evaluation points for simulation. Since our intent in the wind farm maintenance application is to optimize the fleet mix, there is little interest in evaluating the value function for inputs that are known to yield small profits. A reasonable criterion for finding new evaluation points is therefore what is often referred to as expected improvement (EI), which allows closed form expressions for GPs. We present some foundational EI related ideas here; these functional expressions for EI are closely connected to those used later for VOI analysis (Section 4).

Let $v^* = \max\{y_1, \ldots, y_M\}$ denote the optimal value evaluation thus far, over the existing batches of evaluations. EI then considers the following acquisition function,

$$\text{Acq}(v) = \max\{0, v - v^*\}, \tag{11}$$

meaning that an improvement in the function value gives a linear reward. EI is defined as the expected value of this acquisition function. Considering one location only, with function value $v \sim N(m, s^2)$, we have

$$\begin{aligned}\text{EI} &= E[\text{Acq}(v)] = \int_{-\infty}^{\infty} \max\{0, v - v^*\}\, p(v)dv = \int_{v^*}^{\infty} (v - v^*)p(v)dv \\ &= \int_{v^*}^{\infty} vp(v)dv - v^* \int_{v^*}^{\infty} p(v)dv = \int_{\frac{v^*-m}{s}}^{\infty} (m + sz)p(z)dz - v^* \int_{\frac{v^*-m}{s}}^{\infty} p(z)dz \\ &= s\phi(z) + (m - v^*)\Phi(z), \end{aligned} \tag{12}$$

where $z = \frac{m-v^*}{s}$, and $\phi(z)$ is the standard normal density function and $\Phi(z)$ the cumulative distribution function. Moreover, $\int ze^{-\frac{z^2}{2}}dz = -e^{-\frac{z^2}{2}} + \text{const}$ is used in the integration.

The expression for EI in (12) has two components – the first term encourages value exploration where there is large uncertainty because higher levels of s yield larger EI, whereas the second term encourages exploitation where there is a large mean because higher $(m - v^*)$ results in larger EI. If we select only one evaluation point in the next batch, we choose the input alternative that has the largest EI.

Example:

As a continuation of the example from earlier, Figure 1 (bottom) shows the EI after updating the model with realized values at the six evaluation points. The displayed EI illustrates that a natural next evaluation point would be either $a = 85$ or $a = 40$. In practical implementations, a batch evaluation is often combined with some sort of space filling criterion, which prevents the chosen evaluation points to be too close to one another (Schonlau et al. 1998, Chevalier and Ginsbourger 2013). Say, in this illustrative example it would be wasteful to run the simulator for both $a = 84$ and $a = 85$ as they would provide almost identical information.

4. Value of Information Analysis

For many real-world decision situations, a reasonable model with sufficient cogency requires a complex joint distribution over the uncertainties and/or a value function that requires extensive simulations. In such situations, closed-form analytic expressions for VOI as shown in equations (4) and (7) are unavailable. This is illustrated for instance in Eidsvik et al. (2015), who provide numerous practical examples of such situations from the Earth sciences.

In this section, we present a computational approach for VOI analysis that uses a GP to approximate the value function for each alternative and state of uncertainty (fleet mix and failure rate, in our application). The VOI is then approximated by using the estimated values from this GP surrogate model and summing over the discretized domain. This approximation becomes the main task, and is done using formulas similar to EI, for each state of the uncertainty. This procedure facilitates efficient approximation of the VOI for different prior and likelihood models.

4.1. Approximating VOI with GP Surrogates

Suppose that we evaluate the simulator at M points of configurations over alternatives and uncertainty states: $(\boldsymbol{a}_1, \lambda_1), ..., (\boldsymbol{a}_M, \lambda_M)$. As in equation (10), the simulator results are denoted $y_1, \ldots, y_M$. The value function is represented by a GP, after conditioning to the data, with values $\boldsymbol{v}$ having mean $\hat{\boldsymbol{v}} = \boldsymbol{\mu}_M$ and covariance matrix $\boldsymbol{\Sigma}_M$ from equation (10).

The prior value approximation becomes

$$\widehat{\mathrm{PV}} = \max_{\boldsymbol{a}\in\mathcal{A}} \left\{ \sum_{\lambda\in\Lambda} \hat{v}(\lambda, \boldsymbol{a}) p(\lambda) \right\}. \tag{13}$$

We will consider both perfect and imperfect information about the failure rate. For the computation of $\widehat{\mathrm{VOI}}$ with perfect information, we simply plug in the estimated value function $\hat{v}(\boldsymbol{a}, \lambda)$ and prior distribution $p(\lambda)$ to calculate the posterior value in equation (3). For imperfect information, the posterior value is approximated by

$$\widehat{\mathrm{PoV}}(l) = E\left(\max_{\boldsymbol{a}\in\mathcal{A}} \{ E\left(\hat{v}(\boldsymbol{a}, \lambda) \,|\, l \right) \} \right) = \sum_{l} \max_{\boldsymbol{a}\in\mathcal{A}} \left\{ \sum_{\lambda\in\Lambda} \hat{v}(\lambda, \boldsymbol{a}) p(\lambda|l) \right\} p(l). \tag{14}$$

The evaluation points over configurations of alternatives and uncertainties must be chosen wisely to get a reasonable approximation of the VOI. We next discuss sequential approximation of the VOI, where M evaluation points are selected for each batch. As the number of such iterations increases, the quality of the VOI approximation improves because the values get more accurate. In practice, the goal is to use as few evaluations as possible while still maintaining reliable VOI approximations.

4.2. Sequential Approximation of VOI

We suggest improving the approximation of the VOI sequentially, as illustrated in Figure 2. After a batch of simulations are done, we augment the current observation set with these new evaluation points and their values, and update the GP surrogate model. The steps of simulations and model updating are repeated until we reach a stopping criterion for the VOI approximation. At each stage of approximation, the next batch of evaluation points are chosen based on an EI-type criterion similar to equation (12), but now this must be done for each level of uncertainty.

We define the optimal prediction value thus far for fixed uncertainty λ as

$$v^*(\lambda) = \max_{\boldsymbol{a}\in\mathcal{A}} \{ \hat{v}(\boldsymbol{a}, \lambda) \}, \qquad \lambda \in \Lambda. \tag{15}$$

We use an acquisition function

$$\alpha\left(\boldsymbol{a}, \lambda\right) = E\left(\max\{ v(\boldsymbol{a}, \lambda) - v^*(\lambda), 0 \} \right), \tag{16}$$

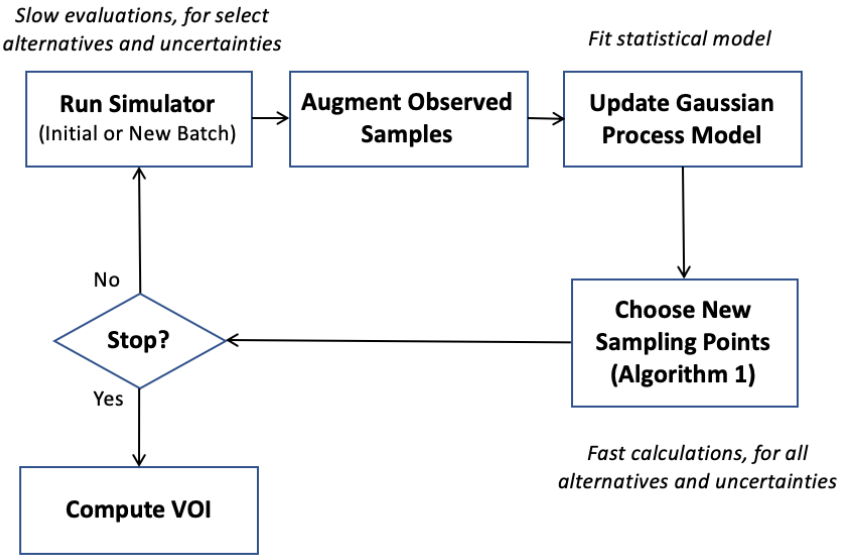

Figure 2 **Flowchart illustrating the sequential approach in Algorithm 2 for approximating the values and the VOI.**

which is the EI for any specified λ uncertainty. By doing so for each uncertainty level, it is straightforward to study sensitivities to different prior and likelihood models on the VOI result. Note that other approaches utilizing properties of the probability mass function $p(\lambda)$ could potentially focus more directly on the VOI expression, and possibly use less evaluation points to yield a good approximation.

Algorithm 1 Generate new points for evaluation

1. Compute $\alpha(\boldsymbol{a}, \lambda)$ for all points using the GP surrogate
2. Initialize $X_{\text{cand}} =$ evaluation points from previous batch evaluations
3. **for each uncertainty level** λ_k, $k = 1, 2, ..., M$
4. $\quad Y_{\text{cand},k} =$ evaluation point for uncertainty λ_k from previous batch evaluations
5. $\quad$ **repeat** (until no more candidates for λ_k)
6. $\quad\quad$ Propose $\boldsymbol{a}_{\text{cand},k} = \text{argmax}_{\boldsymbol{a}}\{\alpha(\boldsymbol{a}, \lambda_k); [\boldsymbol{a}, \lambda_k] \notin Y_{\text{cand},k}\}$
7. $\quad\quad$ **if** $\alpha(\boldsymbol{a}_{\text{cand},k}, \lambda_k) < \epsilon$
8. $\quad\quad\quad$ **return**
9. $\quad\quad$ **elseif** distance$(|\boldsymbol{a} - \boldsymbol{a}_{\text{cand},k}|, |\lambda - \lambda_k|) < \delta \quad \forall [\boldsymbol{a}, \lambda] \in X_{\text{cand}}$
10. $\quad\quad\quad$ **return**
11. $\quad\quad$ **else**
12. $\quad\quad\quad$ $X_{\text{cand}} = \{X_{\text{cand}}, [\boldsymbol{a}_{\text{cand},k}, \lambda_k]\}$, $Y_{\text{cand},k} = \{Y_{\text{cand},k}, [\boldsymbol{a}_{\text{cand},k}, \lambda_k]\}$
13. **return**

Algorithm 1 summarizes the approach for simulator evaluation point selection. The algorithm runs through each level of uncertainty, selecting new points in the batch. There is a tuning parameter for maintaining some distance (as defined by a threshold $\delta > 0$) between evaluation points. This is based on the assumption of a smooth value function, enabling one to avoid the evaluation of multiple points that carry almost identical information. Moreover, if the EI is minuscule (as defined by a threshold $\epsilon > 0$), there is no point in exploring points any further. Hence, there are at most $M = 15$ evaluations per batch.

Algorithm 2 Sequential approximation of the VOI

1. Define
   - Feasible values for decision variables, $\boldsymbol{a}$
   - M feasible values for uncertain variable, λ
2. Obtain initial sample
   - Sample initial points $(\boldsymbol{a}, \lambda)_1, ..., (\boldsymbol{a}, \lambda)_M$
   - Evaluate y_i for inputs $(\boldsymbol{a}, \lambda)_i$ using the simulator, $i = 1, ..., M$
   - $\mathcal{D}_0 = \{(\boldsymbol{a}_i, \lambda_i, y_i)\}_{i=1}^{M}$
   - Fit the GP surrogate model, $\boldsymbol{v} \,|\, \mathcal{D}_0 \sim N(\hat{\boldsymbol{v}}, \boldsymbol{\Sigma}_M)$
3. **repeat until convergence** $b = 1, \ldots$
   - Find new evaluation points as in Algorithm 1
   - Evaluate y_i using the simulator for all new evaluation points
   - Augment $\mathcal{D}_b$ with new observations
   - Fit the GP surrogate model, conditional on all observations $\mathcal{D}_b$

   until stopping criterion
4. Specify distribution of uncertainty $p(\lambda)$ and measurement model $p(l|\lambda)$.
5. Return $\widehat{\text{VOI}} = \widehat{\text{PoV}} - \widehat{\text{PV}}$

Algorithm 2 shows how the VOI is estimated sequentially. We denote the current set of observations by $\mathcal{D}_b$, $b = 0, 1, \ldots$, where the data accumulates through batches of newly obtained evaluation points. We assume that a random set of M points are evaluated for the first time ($b = 0$). At a given stage $b = 1, \ldots,$ of the approximation, the procedure in Algorithm 1 is used to explore areas that are yet to be evaluated, while exploiting promising parts given the currently available information. For the first batch, there is no such information, but the amount of information grows over the remaining stages. The search for the optimal configuration for each failure rate continues until there are no more candidates X_{cand} satisfying the thresholds defined by ϵ and δ in Algorithm 1.

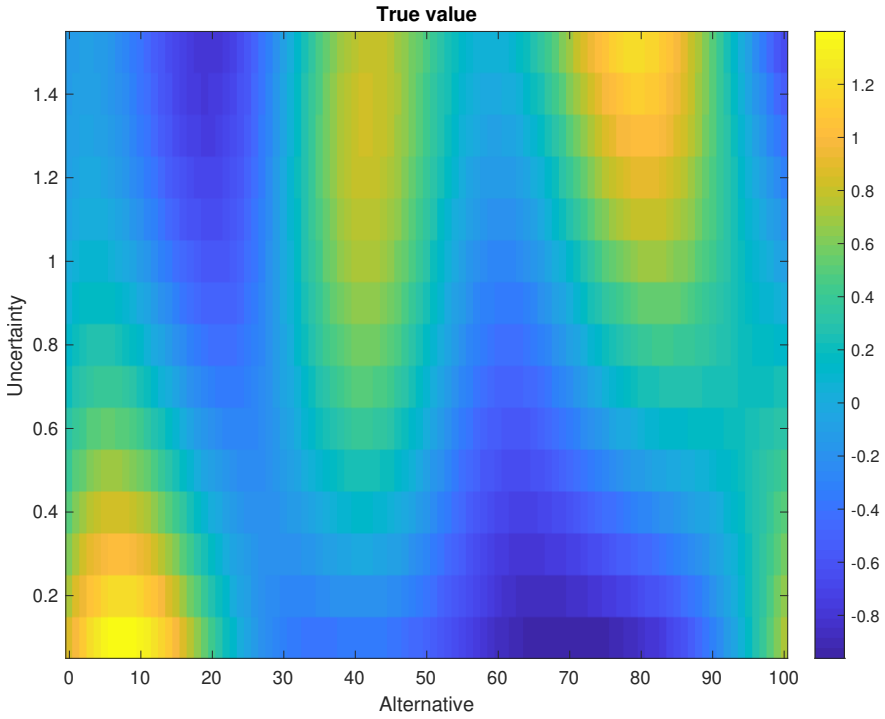

Figure 3 **True value surface for various alternatives and uncertainties.**

Example:

We illustrate the approach using an example that extends the one discussed in Section 4. Figure 3 illustrates the underlying true values as a function of alternatives 1 to 100 on the first axis and uncertainty level from 0.1 to 1.5 on the second axis. For this illustration the optimal alternative for uncertainty level 0.1 is $a = 8$, for uncertainty 1 it is $a = 40$ and for 1.5 it is $a = 80$. There is thus a tendency of higher optimal alternatives when there is larger uncertainty.

The goal is to learn the optimal alternatives for different uncertainties, and doing so using only a small number of evaluation points. This would lead to accurate approximation of the VOI. Here the true underlying values are not computed from a GP, but we use the proposed approach of fitting a GP surrogate model to the evaluations of values in a sequential manner.

In Figure 4, the EI, as calculated for each uncertainty level, is shown over iterations (batch runs). For the earlier evaluation batches, the EI fluctuates a bit because of some surprisingly large evaluations, but when we learn the value surface better, the trend is declining EI over stages. Here there is hardly any distance limit on the evaluation points and we evaluate 15 points at each stage.

Figure 5 shows the mean prediction (left) of value and the associated standard deviation (right), after 20 iterations of the algorithm. We observe that the mean captures the true values shown in Figure 3 reasonably well. The variances are still quite large at locations where the value function is small, such as large uncertainty levels and small-indexed alternatives and low uncertainty and

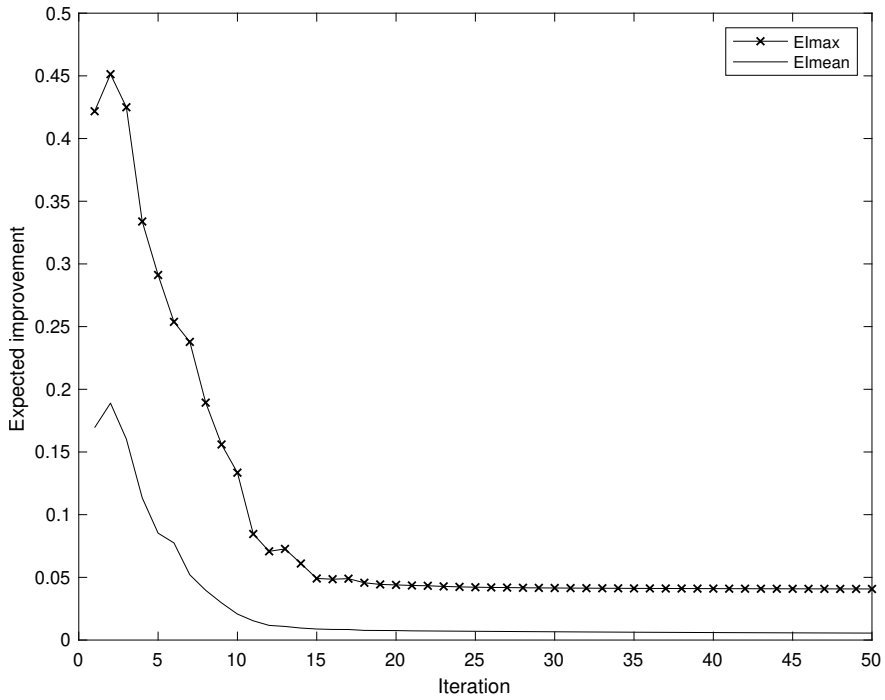

Figure 4 **Expected improvement over iterations. The EI is calculated for each uncertainty level, and then maximized (crosses) and averaged (solid) for all alternatives and all uncertainties.**

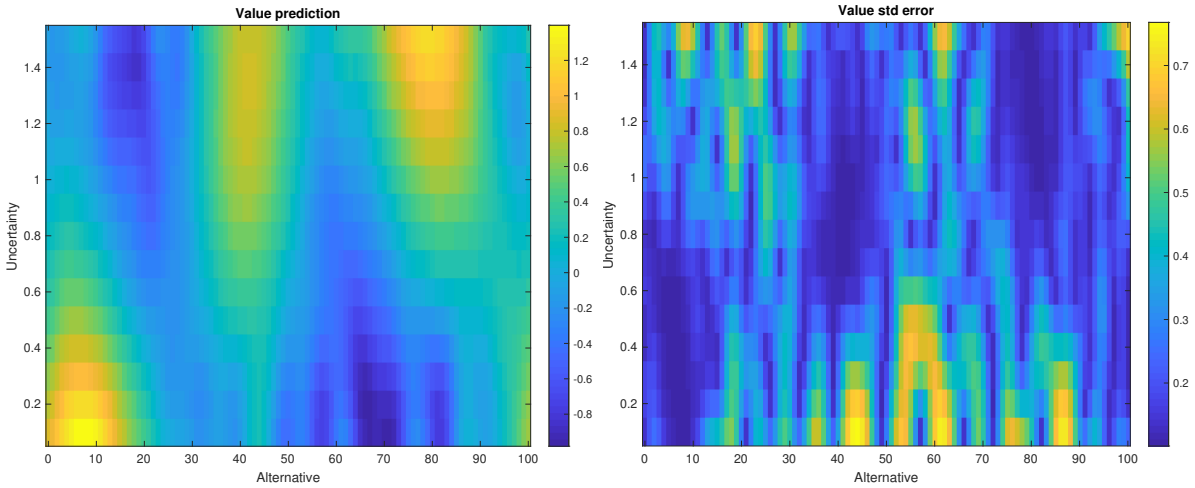

Figure 5 **Prediction (left) and prediction standard deviations (right) of values after 20 iterations of batch evaluations.**

high-indexed alternatives. This occurs because the algorithm focuses its evaluation resources at the locations with largest potential of having high value. There is no point in evaluating points that have low value and/or relatively small uncertainty.

The EI at iteration 20 is shown in Figure 6. Even though there are still some locations with significant EI, it is very small in most locations away from the optimum locations. The EI is also

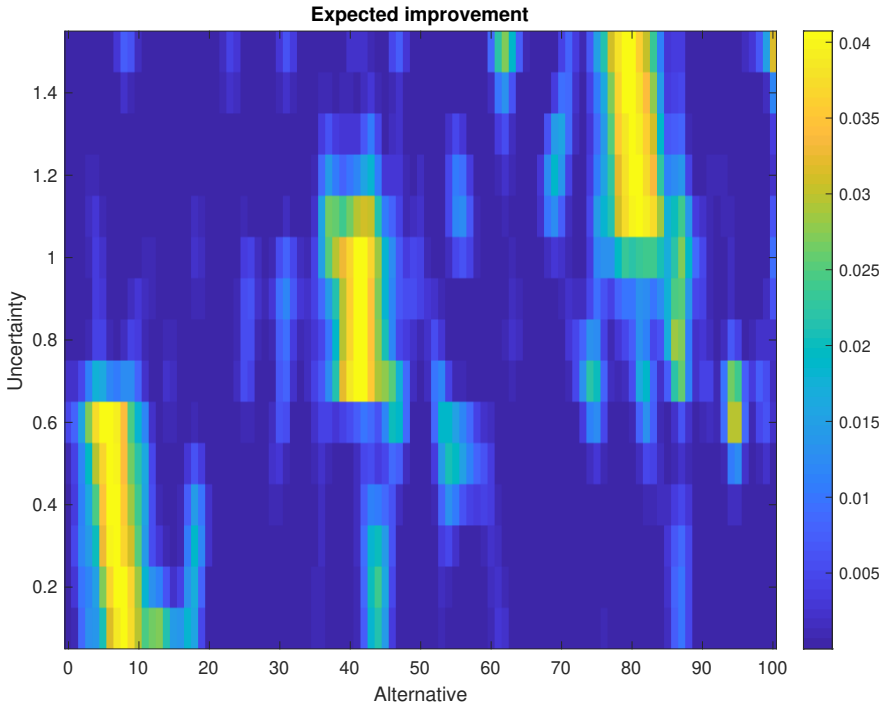

Figure 6 **Expected improvement after 20 iterations of batch evaluations.**

quite small at the optimum locations. For some levels of uncertainty it is however still difficult to make decisions, such as uncertainty $\lambda = 0.6$, where there are several alternatives with significant EI, and it is still unclear which alternative is better. More iterations demonstrate that alternatives 5-10 are the best candidates. Since the algorithm is good at detecting high-value regions for different uncertainty levels and learning their actual values, the VOI approximation turns out to be reasonable. The probability of improvement is still 0.5 at these high-value locations, but because the variance reduces with evaluations, the EI will continue to decline with more evaluations, without really improving the VOI approximation substantially.

5. Case Study for Offshore Wind Farms

We apply the proposed methodology to offshore wind farm O&M. Our focus is on VOI analysis of the turbine failure rate. Others have looked at VOI analysis in this setting, but not using complex simulators as we do here. Seyr and Muskulus (2016) estimate the value of knowing the repair times for wind turbines, for improved maintenance scheduling. For their high-level study, they only consider a small subset of alternatives involving the vessel fleet mix and number of personnel. Colone et al. (2018) study the value of monitoring and early warning systems of failures in wind turbine systems.

The case study presentation is organized as follows: First we describe the decision situation and then motivate the importance of information about the failure rates of turbine components

to optimize operations. Next we present the approximation method and study the properties of the GP surrogate model in the context of the application. Finally, we compare VOI results for various prior models and different levels of accuracy for data gathering, and end by discussing the implications of conducting such VOI analysis.

5.1. O&M for Offshore Wind Farms

There is currently a drive towards building energy producing offshore wind farms because they can be more socially acceptable and less harmful to the environment than their onshore counterpart. O&M costs and potential revenue losses due to turbine downtime can however be large for offshore wind farms, and therefore it is important to plan wisely to optimize strategies. In the current work, we limit scope to an O&M problem where the alternatives involve a vessel fleet with two types of vessels for transferring maintenance personnel to wind turbines: standard crew transfer vessels (CTVs) and more advanced but also more costly surface effect ships (SESs) (Sperstad et al. 2017b). The decision variables are thus: i) a_{CTV} = the number of CTVs, ii) a_{SES} = the number of SESs, and iii) a_p = the number of maintenance personnel. The sets of possible alternatives are respectively:

$$a_p \in \mathcal{A}_p = \{10, 11, ..., 50\}, \;\; a_{CTV} \in \mathcal{A}_{CTV} = \{0, 1, ..., 4\}, \;\; a_{SES} \in \mathcal{A}_{SES} = \{0, 1, ..., 4\}.$$

The cardinality of $\boldsymbol{a} = (a_p, a_{CTV}, a_{SES}) \in \mathcal{A}$ is therefore $41 \cdot 5 \cdot 5 = 1025$. Note that there are of course several other decisions involved in practice, in the context of wind farms: where to place the wind farm, which turbines to use, etc. We assume that they are fixed in our study since we focus solely on O&M strategies.

The main uncertainty is the annual failure rate of wind turbine components:

$$\lambda \in \{0.1, 0.2, ..., 1.5\}.$$

The cardinality of $\lambda \in \Lambda$ is 15. Turbine failures are assumed to follow a homogeneous Poisson process with this average yearly rate λ. Note that in practice, one can model failure rates by distinguishing rates for different components and levels of severity and represent these as separate failure categories in the input data for the simulator. The simulator distinguishes between preventive and corrective maintenance tasks: the former includes annual services for each turbine, while the latter involves tasks related to random failures. For the sake of simplicity, in this study we limit the scope to a failure category of medium severity ("medium repair" from Dinwoodie et al. (2015)).

In theory, it is possible to run the simulator $v(\boldsymbol{a}, \lambda)$ for all possible combinations of vessels and personnel, and in this way find the optimal O&M strategy, for different failure rates. However, the simulation involves complex event-based interactions and it is time-consuming to get profit

values for a given combination of inputs. Hence, in practice, one can only run the simulator for a subset of the possible inputs, and thus it becomes important to guide the evaluation to useful combinations of the states of uncertainties (failure rates) and alternatives of decision variables (vessel and personnel).

5.2. Modeling Failure Rates

Failure rates have previously been shown to greatly impact estimates of energy profits (Dinwoodie et al. 2015). It has also been shown that the optimal selection of the O&M vessel fleet is sensitive to failure rate assumptions so that one should consider reducing the uncertainty in these input data (Sperstad et al. 2017b).

Comprehensive data collection has been carried out to learn the failure rates of wind turbine components (Pfaffel et al. 2017, Artigao et al. 2018). However, it has been shown to be difficult to generalize results (which could also be proprietary), and thus there are various uncertainties pertaining to the failure rate for a given wind farm project. For instance, Scheu et al. (2017) study uncertainties in the distribution of time to failure for a given long-term average failure rate λ. For the purpose of this article, we model the prior uncertainty of the failure rate λ itself, and we next discuss how to model this uncertainty.

Faulstich et al. (2011) analyze the results from a large monitoring survey for onshore wind turbines conducted by Fraunhofer IWES. This survey collected 64,000 maintenance and repair reports from 1500 wind turbines. The result from the analysis of this work concludes that the annual failure rate for minor repairs is 1.8 and 0.6 for major repairs. Here, minor repairs are defined as failures with downtimes less than a day, while a major repair is defined as a failure with downtimes that exceed one day. Carroll et al. (2016) have conducted an analysis of a data set based on ~ 350 offshore wind turbines, but the type of the turbines and the exact age of the turbines and number of wind farms are not provided in the paper for confidentiality reasons. The paper concludes that the annual failure rate for minor repairs is 6.81, for major repair it is 1.17 and 0.28 for major replacement. Dinwoodie et al. (2015) present a reference data set for simulation of O&M tasks for offshore wind farms. Five different failure categories are used here: manual reset, minor repair, medium repair, major repair and major replacement. The proposed values for the annual failure rates are 7.5 for manual reset, 3.0 for minor repair, 0.28 for medium repair, 0.04 for major repair and 0.08 for major replacement.

From the references above, we note that there is no consensus in the literature on how failure categories should be defined. For references with comparable categories, the value of the failure rate also appears to vary with the data basis of the reference. Our prior assessment in $p(\lambda)$ is loosely based on the rates provided in the literature, and we focus on the medium repair failure

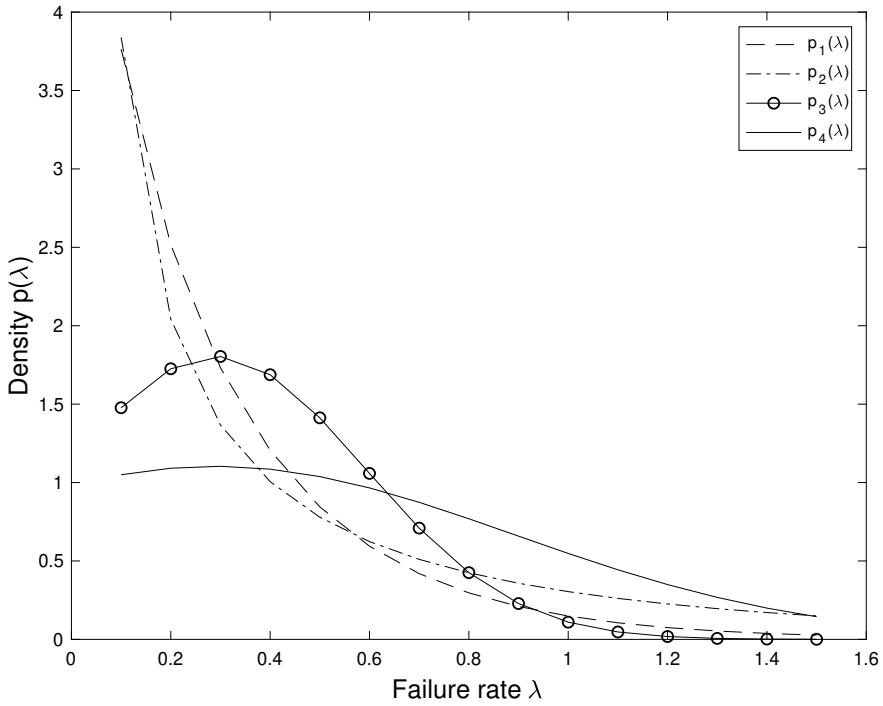

Figure 7 **Plot of the suggested distributions for the uncertain failure rate, λ.**

rate as defined in Dinwoodie et al. (2015). We hence discuss sensitivity to results from four different distributions for the failure rate parameter:

$$p_1(\lambda) = \text{Gamma}(0.9, 0.3),\ \ p_2(\lambda) = \text{Gamma}(0.2, 1.3),\ \ p_3(\lambda) = N(0.28, 0.3^2),\ \ p_4(\lambda) = N(0.28, 0.6^2),$$

where the first argument in the gamma density function denotes the shape parameter while the second is the scale parameter. The distributions are truncated to lie in the interval $[0.1, 1.5]$ and discretized to $\{0.1, \ldots, 1.5\}$. The four probability mass functions are plotted in Figure 7. The mean is 0.28 in all distributions, which is the failure rate for a medium type repair suggested by Dinwoodie et al. (2015). The standard deviation for models p_1 and p_3 is 0.3, while it is 0.6 for p_2 and p_4.

For the other input parameters required by the simulator for the case study, we base ourselves on the reference data sets in Dinwoodie et al. (2015) and Sperstad et al. (2017b). For each evaluation, five Monte Carlo realizations of weather and physical conditions are used. Each realization corresponds to time series of correlated wind speed and wave height data over the year with hourly resolution and times of failure for all turbines over the same period. The same weather realizations are used for each evaluation to reduce the variance in the difference between simulator outputs for different evaluation points.

5.3. Approximation Steps

We gain insight by studying the optimization process and the EI at different stages. Since the value function has four input variables, it is not easily visualized. We will, therefore, consider subsets

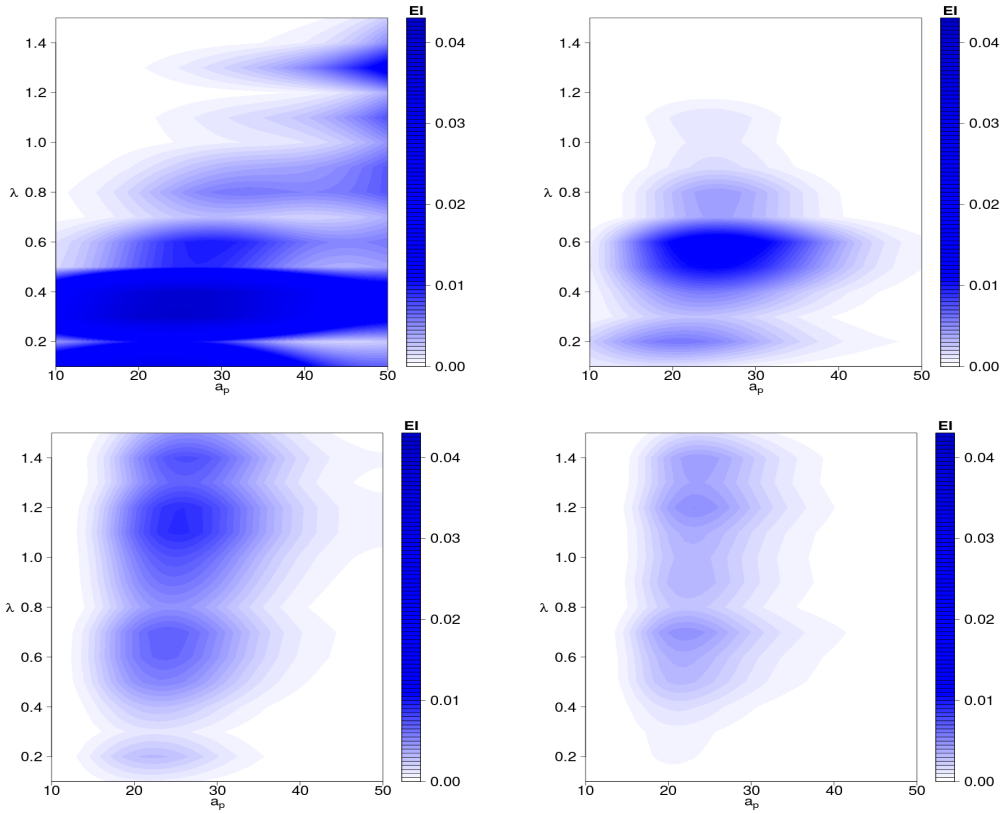

Figure 8 **Relative expected improvement at stages 1 (upper left), 5 (upper right), 10 (lower left) and 20 (lower right) of the optimization process for** $(a_{CTV}, a_{SES}) = (0, 2)$.

of the input space, where the vessel alternatives, a_{CTV} and a_{SES} are fixed. The critical distance between subsequent evaluation points is here set to

$$\text{distance}(\boldsymbol{a}, \boldsymbol{a}', \lambda, \lambda') = |a_p' - a_p| + |a_{CTV}' - a_{CTV}| + |a_{SES}' - a_{SES}| + 10 \cdot |\lambda' - \lambda| > \delta,$$

which leads to some separation of evaluation points.

Figure 8 shows contour plots of the relative EI for the points with $(a_{CTV}, a_{SES}) = (0, 2)$ plotted at different stages in the optimization process. The relative EI is the ratio between the EI and the current best observation thus far. In the upper left corner, we see that there are many points that are candidates for being the maximum. Most of these points are for low values of λ. Points with high a_p at this stage are assumed to be promising, but in the following iterations these points are discarded. We see that the most promising points move towards lower values of a_p.

Figure 8 also demonstrates that we discard many more points than we evaluate since only 15 points are evaluated in each iteration. This is what we desire – to minimize the number of evaluations in the simulator and still find good solutions.

When the relative EI is lower than 0.001 for all feasible points, we choose to terminate the algorithm, which provides an estimate for v. In total 50 iterations and 499 simulator evaluations

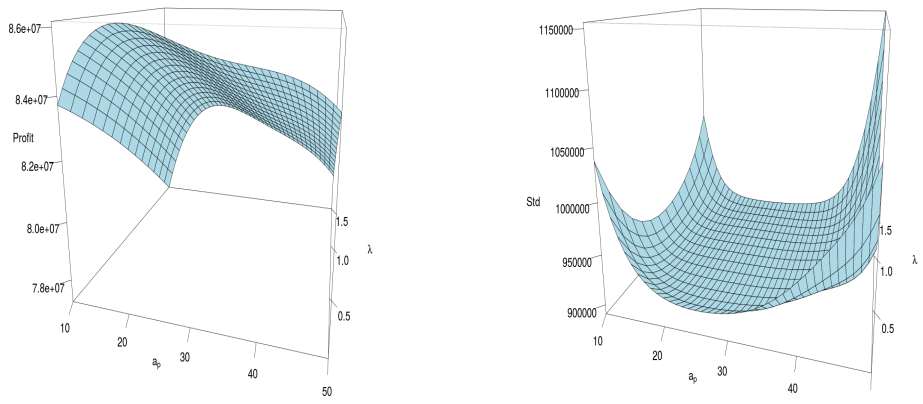

Figure 9 **Estimated value function $\widehat{v}(\lambda, a_p, a_{CTV} = 0, a_{SES} = 2)$ and associated standard deviation (in GBP).**

were required, meaning that the simulator is run less than 15 times as the iterations increase. By 499 evaluations, there is a substantial reduction from the number of feasible points, 15375. Figure 9 depicts the estimated posterior mean and standard deviation for $(a_{CTV}, a_{SES}) = (0, 2)$. The estimated value function (left-hand side) is smooth and the shape is what we would expect – decreasing when λ is large. For $a_p > 24$, the profit decays monotonically, which is again what we expect since each SES only has room for 12 maintenance personnel. This means that when the number of personnel is more than 24, this only results in additional costs. The posterior standard deviation (right-hand side) should be lower in the areas that are well explored, and higher elsewhere. We notice that the areas that had a significant relative EI are the same that have low uncertainty. Note also that the uncertainty is high at points that are unlikely to be candidates for maximum. Thus, promising areas are well explored and less promising areas are not, as intended.

The computation time of the simulator is around 40 seconds per evaluation. In comparison, the GP updating equations and EI calculations, done for all alternatives and failure rates, take less than a second. With careful likelihood tuning of correlation decay parameters ϕ, at each batch, the BO takes some more time, but even so it is orders of magnitude faster than the simulator evaluations.

5.4. GP Model Validity

The parameters in the GP model are estimated based on the initial batch of data, and updated at subsequent batches. The final estimates of the correlation decay parameters are $\phi_p = 2915$, $\phi_{CTV} = 11.9$, $\phi_{SES} = 3.4$ and $\phi_\lambda = 37$, meaning that two value evaluations that differ by one in a_p are more correlated than the ones that differ by one vessel or rate. A small change in the number of personnel should not affect the overall profit much. Changing the number of vessels might lead to large losses either because there are too few vessels available to transport personnel to the wind farm, or because there are too many vessels so that it becomes an unnecessary additional expense.

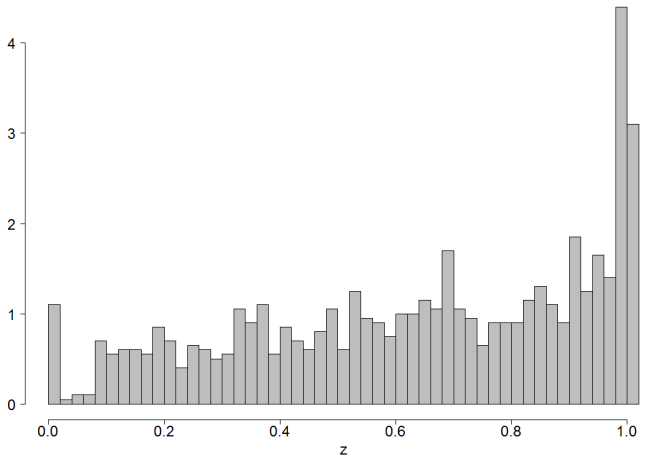

Figure 10 Histogram of the empirical percentiles in the predictive cumulative Gaussian probability distribution.

We study the GP modeling assumption by comparing new observations and its predictive distribution. Denote a new simulator observation by y, with predictive cumulative distribution function $F(y) \in (0,1)$. In our case, this is obtained from the fitted Gaussian, given all currently available evaluations. When a model is correct, the empirical percentiles of new observations should be more or less uniform. We study this empirical percentile for each evaluation in every batch. A histogram for this is provided in Figure 10. Overall the fit to the uniform seems to be good, but we see that there is a spike near zero and a slight overweight of large observations. From closer inspection, the extreme observations tend to occur in areas where we have few observations, often having many vessels and lots of available personnel, but a low failure rate. It is possible that there are heavier tails here than what is being captured by the GP surrogate model. Note also that the evaluations are selected from highest EI, conditional on the previous evaluations, and even though the marginal predictive distribution is Gaussian according to the model, the approach gives non-random sampling of evaluation points.

5.5. Results

Table 1 shows the optimal configurations, as suggested by the fitted GP, for all feasible values of the failure rate λ. As expected, the value function $\widehat{v}$ decays as the failure rate increases. There are two different vessel configurations represented in these results: $(a_{CTV}, a_{SES}) = (0,1)$ and $(a_{CTV}, a_{SES}) = (0,2)$. For low values of λ, one vessel is enough, while higher failure rate means that an additional vessel is required to reduce downtime for the wind farm sufficiently to ensure high profits. We see that the optimal configuration lies in the areas that had a high relative EI in Figure 8. We note that the number of CTV is always 0. This could have simplified the analysis, but it was not evident to us before conducting the analysis. However, from the perspective of the decision maker, this

result of the analysis means that a decision to exclude CTV alternatives from the vessel fleet would be robust with respect to the uncertainty in the failure rate λ.

Table 1 The estimated optimal configuration for each feasible value of the failure rate, λ. Here, $\hat{v}$ is the estimated posterior mean and $\sigma(\hat{v})$ is the estimated posterior standard deviation in the GP (in Mill GBP).

a_{CTV}	0	0	0	0	0	0	0	0	0	0	0	0	0	0	0
a_{SES}	1	1	1	1	1	2	2	2	2	2	2	2	2	2	2
a_p	12	12	12	12	12	22	22	22	22	22	23	23	23	24	24
λ	0.1	0.2	0.3	0.4	0.5	0.6	0.7	0.8	0.9	1.0	1.1	1.2	1.3	1.4	1.5
$\hat{v}$	87.0	86.7	86.3	85.9	85.3	84.7	84.4	84.1	83.7	83.4	83.1	82.7	82.4	82.0	81.7
$\sigma(\hat{v})$	0.90	0.90	0.90	0.90	0.90	0.89	0.89	0.89	0.89	0.89	0.89	0.89	0.89	0.89	0.90

The optimal O&M strategies without information about the failure rates are listed in Table 2 for the four distributions for λ under consideration. The optimal strategies and the associated PV are found by using (13). Note that $\widehat{v}$ that is plugged into this equation corresponds to the posterior mean in the GP, at the final iteration of Algorithm 2. We see that the distributions with the highest variance yield the lowest PV and the distributions with lowest variance yield the highest PV. The optimal configurations suggested by the distributions agree well with Table 1. For $\lambda \leq 0.5$, the optimal configuration is $(a_p, a_{CTV}, a_{SES}) = (12, 0, 1)$, which is reasonable as there is little demand for maintenance personnel. Most of the probability mass for the two distributions with low variance are for $\lambda \leq 0.5$, so that even though the configuration $(12, 0, 1)$ is sub-optimal for $\lambda > 0.5$, this is not given much weight. The optimal configurations suggested for the distributions with high variances have both two vessels, since a high λ here is assumed to be more likely.

Table 2 Summary of optimal O&M strategy without additional knowledge about the failure rate for the four distributions under consideration. Prior value is in Mill GBP.

Distribution	$p_1(\lambda)$	$p_2(\lambda)$	$p_3(\lambda)$	$p_4(\lambda)$
a_p	12	21	12	22
a_{CTV}	0	0	0	0
a_{SES}	1	2	1	2
PV	85.9	85.1	85.8	84.7

The VOI for perfect information is computed using $\max_{\boldsymbol{a} \in \mathcal{A}} \{\widehat{v}(\lambda, \boldsymbol{a})\}$ listed in Table 1 for all λ and the prior values listed in Table 2. The PoV and VOI for the four distributions under consideration are summarized in Table 3. As expected, the VOI is largest for the distributions with highest variance, where the gamma distribution yields the overall highest VOI.

Table 3 Estimated PoV and VOI (in Mill GBP) for perfect information for the four distributions of the failure rate under consideration.

Distribution	$p_1(\lambda)$	$p_2(\lambda)$	$p_3(\lambda)$	$p_4(\lambda)$
PoV	86.1	85.7	85.9	85.1
VOI	0.21	0.53	0.10	0.35

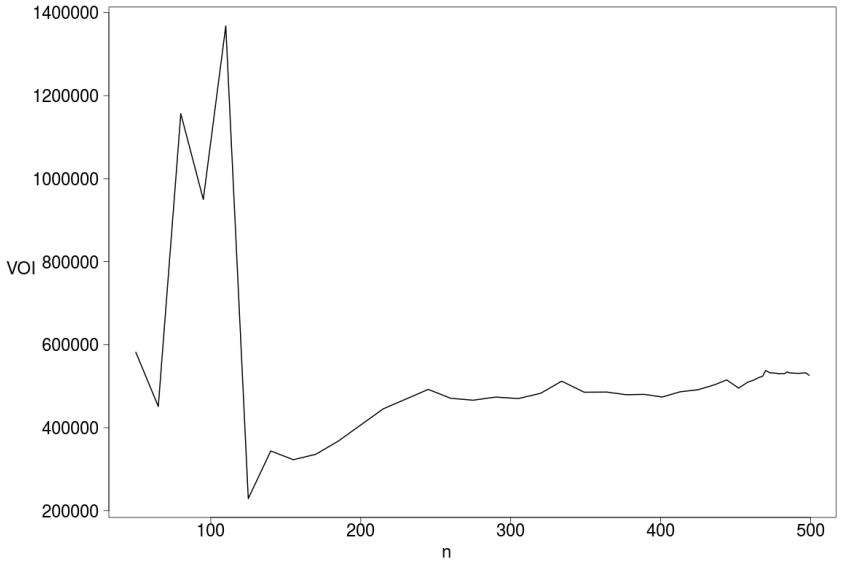

Figure 11 The estimated VOI (in GBP) as a function of the number of simulations.

The PoV for imperfect information is computed by using equation (14) and the four proposed distributions for λ. For sensitivity analysis, we will compute the VOI for three levels of measurement noise in the failure rate, as characterized by the likelihood $p(l|\lambda)$. We let q be the probability that measurement $l = \lambda$, while $p = (1-q)/2$ is the probability that $l = \lambda \pm \Delta$, with $\Delta = 0.1$ being the grid cell width for the discretized domain of failure rates. The result is summarized in Table 4. Comparing Table 4 and Table 3, we note that VOI values are consistently higher for perfect information. For $q = \frac{9}{10}$ and $p = \frac{1}{20}$ the differences between imperfect and perfect information in VOI are rather small. The differences get larger when q decreases and p increases, but the estimates of VOI are still comparably high.

Table 4 Estimated PoV and VOI (in Mill GBP) for imperfect information for the four distributions of the failure rate under consideration.

q	9/10				2/3				1/3			
Distribution	$p_1(\lambda)$	$p_2(\lambda)$	$p_3(\lambda)$	$p_4(\lambda)$	$p_1(\lambda)$	$p_2(\lambda)$	$p_3(\lambda)$	$p_4(\lambda)$	$p_1(\lambda)$	$p_2(\lambda)$	$p_3(\lambda)$	$p_4(\lambda)$
PoV	86.1	85.7	85.9	85.1	86.1	85.7	85.9	85.1	86.1	85.7	85.9	85.1
VOI	0.20	0.52	0.10	0.35	0.20	0.52	0.09	0.35	0.20	0.52	0.09	0.34

Finally, we investigate the precision of the VOI estimate over iterations of the approximation procedure. This is shown for $p_2(\lambda)$. The evolution of $\widehat{\text{VOI}}$ with the number of simulations n is shown in Figure 11. We observe that the VOI estimate changes a lot early on, but then stabilizes as the number of simulations grows. For simulation numbers $n > 250$, there are very small changes in $\widehat{\text{VOI}}$ which suggests that our estimate for VOI has stabilized.

5.6. Discussion

The key observations from the VOI analysis are:

- The prior distributions for λ with the heaviest tails and large variability resulted in the highest VOI.
- The VOI of imperfect information is relatively large compared with that of perfect information.
- The estimate of VOI converged over the number of evaluations during the approximation procedure, and the number of simulator runs was reduced by a factor of about 30 compared to the number of feasible points.

Even though the estimated VOI is small compared with the overall profits, it could be appreciable compared with the O&M budget of the cost center. In particular, VOI analysis is conducted to study information gathering opportunities. In this setting, the VOI should be compared with the costs of getting information about the failure rate of turbines. In practice, this could entail that the wind farm developer make further efforts to scrutinize the data basis and assumptions underlying the failure rate input data, either involving the knowledge and judgement of in-house experts or by procuring external consultancy services. It is not possible in practice to obtain perfect information about the failure rate, but the results above demonstrate how reducing the failure rate uncertainty would be valuable nevertheless. The estimated VOI can also guide additional efforts that could be made by the decision maker during negotiations with wind turbine manufacturers or in learning about the operational experience from comparable operational wind farm projects.

6. Closing Remarks

VOI analysis is an important part of the decision analysis process. The issue of efficiently computing the VOI of uncertainties in complex decision situations that require the use of expensive simulators is pervasive, applicable across many industries. In this paper, we have proposed an approach that uses BO with a GP surrogate model of a computationally expensive simulator to estimate VOI. When optimizing the value function, we only provided input-output relations and the feasible range of the variables. We used the surrogate GP model to find favorable regions in the input space. Our analysis suggests that a GP can be a suitable surrogate model and that the modified EI acquisition function that was deployed could indeed be efficient by reducing the number of simulator runs.

Our methods are motivated by and applied on a relevant decision situation in the O&M of an offshore wind farm. Here the optimal strategy is sensitive to the level for the uncertain failure rate of wind turbines, and the decision maker is interested in estimating the value of knowing the failure rate. By defining the value function as the profit for a given O&M strategy, we can search for favorable strategies by optimizing this function. Results indicate that BO was able to find favorable O&M strategies. VOI analysis conducted for four cases of distributions for the failure rate confirms

the substantial value of the information, and more specifically, provides guidance around the extent of additional research that would be worthwhile for the decision maker.

There are numerous ways to make the modeling and subsequent analysis even more realistic and potentially useful for decision makers involved in O&M for offshore wind farms. One way is to consider several other uncertain variables involved in the decision situation for which the VOI could be estimated. For instance, information about the wave height could be valuable since the O&M vessels are unable to safely transfer maintenance personnel to offshore wind turbines when the waves become too high. One could also distinguish between failure rates for different components or different levels of severity, and estimate VOI for these uncertainties separately or jointly. Another practical extension is to include more decision variables in the model. For our case study we only considered a subset of the possible decision variables for O&M. A natural extension of this study is therefore to also include decision variables such as the location of the O&M base (e.g. on an offshore accommodation platform) and more O&M vessel concepts (e.g. other vessels or helicopters). This is particularly relevant for the new generation of offshore wind farms currently under development, for which the increasing size and increasing distance to shore make the decision situation even more complex.

We highlight that there are limitations and therefore room for improvement pertaining to the computational methodology. Some of the assumptions we made when specifying the GP, for instance assuming the same covariance structure over the whole feasible domain, could be over-simplifications in some situations. By partitioning the input space into disjoint regions, one might achieve more accurate estimates of the uncertainty. Furthermore, for more efficient optimization of the value function, we could let the minimum relative improvement ϵ be a function of the failure rate. We could then adjust the selection so that points with rates that are unlikely, based on the probability distribution of the failure rate, be subjected to less exploration. Although this would yield a less accurate estimate of the value function for some values of the rate, it would likely not affect the overall estimation of VOI significantly. We also assumed a risk neutral decision maker for the analysis here; other risk attitudes are certainly relevant in practice, and some of the analysis could perhaps also be computationally tractable for a decision maker with an exponential utility function, given the analytical GP equations, see e.g. Bickel (2008) and Bhattacharjya et al. (2013).

VOI analysis for complex decision models often raises computational issues in practice. We have shown that the use of surrogate models together with methods from BO could lead to significant computational savings. We suspect that advances in research that tackle these challenges head-on could promote and motivate the use of decision analytic notions such as VOI in practical organizational settings. For instance, the explicit incorporation of complex simulators in the decision

analytic model brings together cross-functional teams, making the analysis more powerful and likely more acceptable and appreciated by the organization's key decision makers.

References

Artigao, E., Martín-Martínez, S., Honrubia-Escribano, A., Gómez-Lázaro, E., 2018. Wind turbine reliability: A comprehensive review towards effective condition monitoring development. Applied Energy 228, 1569–1583.

Asher, M.J., Croke, B.F., Jakeman, A.J., Peeters, L.J., 2015. A review of surrogate models and their application to groundwater modeling. Water Resources Research 51, 5957–5973.

Bhattacharjya, D., Eidsvik, J., Mukerji, T., 2013. The value of information in portfolio problems with dependent projects. Decision Analysis 10, 341–351.

Bickel, J.E., 2008. The relationship between perfect and imperfect information in a two-action risk-sensitive problem. Decision Analysis 5, 116–128.

Bierlaire, M., 2015. Simulation and optimization: A short review. Transportation Research Part C: Emerging Technologies 55, 4–13.

Blum, D., Paté-Cornell, M., 2016. Probabilistic warnings in national security crises: Pearl Harbor revisited. Decision Analysis 13, 1–25.

Bratvold, R., Bickel, J., Lohne, H., 2009. Value of information in the oil and gas industry: Past, present, and future. SPE: Reservoir Evaluation and Engineering 12, 630–638.

Carroll, J., McDonald, A., McMillan, D., 2016. Failure rate, repair time and unscheduled O&M cost analysis of offshore wind turbines. Wind Energy 19, 1107–1119.

Chevalier, C., Ginsbourger, D., 2013. Fast computation of the multi-points expected improvement with applications in batch selection, in: International Conference on Learning and Intelligent Optimization, Springer. pp. 59–69.

Colone, L., Reder, M., Dimitrov, N., Straub, D., 2018. Assessing the utility of early warning systems for detecting failures in major wind turbine components. Journal of Physics: Conference Series 1037, 032005.

Dinwoodie, I., Endrerud, O.E.V., Hofmann, M., Martin, R., Sperstad, I.B., 2015. Reference cases for verification of operation and maintenance simulation models for offshore wind farms. Wind Engineering 39, 1–14.

Eidsvik, J., Mukerji, T., Bhattacharjya, D., 2015. Value of Information in the Earth Sciences: Integrating Spatial Modeling and Decision Analysis. Cambridge University Press.

Faulstich, S., Hahn, B., Tavner, P.J., 2011. Wind turbine downtime and its importance for offshore deployment. Wind Energy 14, 327–337.

Frazier, P.I., Wang, J., 2016. Bayesian optimization for materials design, in: Information Science for Materials Discovery and Design. Springer, pp. 45–75.

Ghanem, R., Higdon, D., Owhadi, H., 2017. Handbook of Uncertainty Quantification. Springer.

Gramacy, R.B., 2016. lagp: Large-scale spatial modeling via local approximate Gaussian processes in R. Journal of Statistical Software 72, 1–46.

Gramacy, R.B., Lee, H.K., 2009. Adaptive design and analysis of supercomputer experiments. Technometrics 51, 130–145.

Hofmann, M., 2011. A review of decision support models for offshore wind farms with an emphasis on operation and maintenance strategies. Wind Engineering 35, 1–15.

Hofmann, M., Sperstad, I.B., 2013. NOWIcob – a tool for reducing the maintenance costs of offshore wind farms. Energy Proc. 35, 177–186.

Howard, R.A., 1966. Information value theory. IEEE Transactions on Systems Science and Cybernetics 2, 22–26.

IRENA, 2018. Renewable Power Generation Costs in 2017. Report. International Renewable Energy Agency. URL: `https://www.irena.org/-/media/Files/IRENA/Agency/Publication/2018/Jan/IRENA_2017_Power_Costs_2018.pdf`.

Keisler, J., Collier, Z., Chu, E., Sinatra, N., Linkov, I., 2014. Value of information analysis: The state of application. Environment Systems and Decisions 34, 3–23.

Matheson, J.E., 1968. The economic value of analysis and computation. IEEE Transactions on Systems Science and Cybernetics 4, 325–332.

Merrick, J., 2009. Bayesian simulation and decision analysis: An expository survey. Decision Analysis 6, 222–238.

Oakley, J.E., O'Hagan, A., 2004. Probabilistic sensitivity analysis of complex models: A Bayesian approach. Journal of the Royal Statistical Society: Series B (Statistical Methodology) 66, 751–769.

Owen, N., Challenor, P., Menon, P., Bennani, S., 2017. Comparison of surrogate-based uncertainty quantification methods for computationally expensive simulators. SIAM/ASA Journal on Uncertainty Quantification 5, 403–435.

Pawar, R.J., Bromhal, G.S., Chu, S., Dilmore, R.M., Oldenburg, C.M., Stauffer, P.H., Zhang, Y., Guthrie, G.D., 2016. The national risk assessment partnership's integrated assessment model for carbon storage: A tool to support decision making amidst uncertainty. International Journal of Greenhouse Gas Control 52, 175–189.

Pfaffel, S., Faulstich, S., Rohrig, K., 2017. Performance and reliability of wind turbines: A review. Energies 10, 1904.

Queipo, N.V., Haftka, R.T., Shyy, W., Goel, T., Vaidyanathan, R., Tucker, P.K., 2005. Surrogate-based analysis and optimization. Progress in Aerospace Sciences 41, 1–28.

Rasmussen, C.E., 2004. Gaussian processes in machine learning, in: Advanced Lectures on Machine Learning. Springer, pp. 63–71.

Roustant, O., Ginsbourger, D., Deville, Y., 2012. DiceKriging, DiceOptim: Two R packages for the analysis of computer experiments by Kriging-based metamodeling and optimization. Journal of Statistical Software 51, 1–55.

Sacks, J., Welch, W.J., Mitchell, T.J., Wynn, H.P., 1989. Design and analysis of computer experiments. Statistical Science , 409–423.

Scheu, M.N., Kolios, A., Fischer, T., Brennan, F., 2017. Influence of statistical uncertainty of component reliability estimations on offshore wind farm availability. Reliability Engineering & System Safety 168, 28–39.

Schonlau, M., Welch, W.J., Jones, D.R., 1998. Global versus local search in constrained optimization of computer models. Lecture Notes-Monograph Series 34, 11–25.

Seyr, H., Muskulus, M., 2016. Value of information of repair times for offshore wind farm maintenance planning, in: Journal of Physics: Conference Series, IOP Publishing. p. 092009.

Seyr, H., Muskulus, M., 2019. Decision support models for operations and maintenance for offshore wind farms: A review. Applied Sciences 9. doi:10.3390/app9020278.

Snoek, J., Rippel, O., Swersky, K., Kiros, R., Satish, N., Sundaram, N., Patwary, M., Prabhat, M., Adams, R., 2015. Scalable bayesian optimization using deep neural networks, in: International Conference on Machine Learning, pp. 2171–2180.

Sperstad, I.B., Kolstad, M.L., Hofmann, M., 2017a. Technical documentation of version 3.3 of the NOWIcob tool. SINTEF Energy Research. Report no. TR 7374, v.4.0 .

Sperstad, I.B., Stålhane, M., Dinwoodie, I., Endrerud, O.E.V., Martin, R., Warner, E., 2017b. Testing the robustness of optimal access vessel fleet selection for operation and maintenance of offshore wind farms. Ocean Engineering 145, 334–343.

Strong, M., Oakley, J.E., Brennan, A., Breeze, P., 2015. Estimating the expected value of sample information using the probabilistic sensitivity analysis sample: A fast, nonparametric regression-based method. Medical Decision Making 35, 570–583.

Tavner, P., 2012. Offshore Wind Turbines: Reliability, Availability and Maintenance. The Institution of Engineering and Technology.

Welte, T.M., Sperstad, I.B., Halvorsen-Weare, E.E., Netland, Ø., Nonås, L.M., Stålhane, M., 2018. Operation and maintenance modelling. Offshore Wind Energy Technology , 269–304.

Yokota, F., Thompson, K., 2004. Value of information literature analysis: A review of applications in health risk management. Medical Decision Making 24, 287–298.